2022 International Conference on Indoor Positioning and Indoor Navigation (IPIN), 5 - 7 Sep. 2022, Beijing, China

A Metric for Quantifying UWB Ranging Error Due to Clock Drifts

Haige Chen
Georgia Institute of Technology, Atlanta, USA
hchen425@gatech.edu

Ashutosh Dhekne
Georgia Institute of Technology, Atlanta, USA
dhekne@gatech.edu

***Abstract*—Wireless ranging, where two or more wireless devices determine their relative distance by exchanging messages, is a fundamental primitive in short-range distance measurements and localization. These methods are used by fine-time measurement in WiFi, and ultra-wideband (UWB) radios which is seeing an uptick in the smartphone market. Since ranging depends on accurate timestamps, the clock drifts between devices is an important consideration that affects ranging precision. Several applications have been proposed in the short-range localization context with their own ranging protocols and almost all of them perform clock-drift analysis to assess the quality of the protocol and ranging formulation. Although this is standard practice, there lacks a way to quantify and compare the extent of clock-drift introduced measurement errors. In this work, we introduce a metric based on numerical simulations that enables direct comparisons across schemes, and demonstrate how it helps analyze distance measurement errors.**

***Index Terms*—ranging, UWB localization, clock drift, error metric**

I. Introduction

Indoor localization is experiencing an upward trend driven by numerous applications in indoor navigation, context aware recommendations, object and people tracking etc. The bulk of location related services today rely on GPS. However, there are limits to the capabilities of GPS. It fails to work indoors, and does not have fine-grained precision. Mobile manufacturers already acknowledge these limitations and hence have gravitated towards additional means of localization fusing various sources of information to provide higher precision localization. The class of *short-range localization* is slowly taking hold, as manifested by the incorporation of WiFi fine-time measurement and ultra-wideband (UWB) radios in newer smartphone offerings by Apple [1], Samsung [2], and Mi [3], and full Android stacks being developed by Google [4]. Short-range precise localization provides context-awareness to IoT devices and brings in new application level functionalities on the smartphone.

Short-range localization is rooted in trilateration performed via a distance measurement primitive called **wireless ranging**. Theoretically, ranging can be performed in any signal modality as long as precise timestamping of signal transmission and arrival times can be achieved. Especially, ranging-based localization had a huge success in ultra-wideband (UWB) systems [5], exploiting the fact that a large bandwidth (up to ~ 1.3 GHz) allows transmission of fast rising pulses, which enables precise timestamping of signal reception. Conceivably, the 5G and 6G systems, with large available bandwidths (sometimes over 2 GHz), have the potential to unlock ultra-high-precision ranging based localization. Recent works [6], [7] have shown millimeter-level ranging precision for 60 GHz systems.

978-1-7281-6218-8/22/31.00 © 2022$IEEE$

Acknowledging this need for short-range localization, and the myriad requirements of IoT devices (such as whether the device itself requires the location or the infrastructure requires the devices' location), several ranging protocols have been proposed. A key component affecting all wireless ranging protocols is the ability to compensate for the *difference in the clocks* on all participating devices, and the ability to compensate for the *drifting of these clocks*. These clock effects imbibe fundamental precision and robustness limitations on the protocols. Yet, as far as we are aware, there is no clear way to compare the precision and robustness of different ranging schemes. Of course, almost every new ranging scheme shows the effect of clock drifts on its precision, many even perform empirical analysis. However, ranging schemes should not be just compared on the precision scale. They must also be compared on the robustness scale. Loosely speaking, we define robustness of a ranging scheme as the tolerance of a scheme to perturbations in the relative timings of the various messages exchanged between ranging devices. Robustness is such an important feature that the IEEE 802.15.4 standard was modified to adopt a newer formulation that was more resilient to timing variations in the message exchange, while the best case precision remains unaltered in IEEE 802.15.4z [8].

The purpose of this work is not to propose a new ranging scheme or even to survey existing protocols. Instead, we aim to *create a metric that will aid researchers compare different ranging schemes*. While ideally all schemes try to find the propagation delay between two ranging devices, since the underlying clock is unstable, measured propagation delay deviates significantly from the ideal value. This work is an attempt to articulate the expected deviation from the ideal propagation delay, and the scheme's reliance on timing restrictions on the messages exchanged by a device pair.

Our proposed metric takes as input various timing parameters of a scheme and the formulation used by that scheme. It then produces two numerical outputs corresponding to the expected precision and the expected robustness of the scheme. To simplify the task of executing our metric

on new schemes for researchers, we have provided the code and example files for several existing ranging schemes at https://www.mathworks.com/matlabcentral/fileexchange/81798-e-g-metric-for-quantifying-clock-drift-error-in-uwb-ranging.

The rest of this paper is organized as follows. We begin with a short related work section describing how various ranging schemes treat the expected precision and variations in clock-drifts. We then show the methodology for clock-drift analysis for several schemes to prime the reader with the requisite background on the variety of ranging schemes. We then present the details of our metric called the E-G metric, followed by a E-G comparison of 7 ranging schemes, leading to a plot with ranging schemes.

A. Related Work

Many works that present a new ranging scheme mathematically analyse the error introduced by clock-drifts [5], [9]–[11]. Other works dedicated just to clock-drift error characterization also exist: The authors of [12] study clock drift error for four well-known ranging schemes, and compare them analytically and numerically. Authors of [13] examine clock drift induced error in eight positioning schemes: four Time-of-Arrival (ToA) and four Time-Difference-of-Arrival (TDoA) schemes, and deduce their error performance. However, no generalized metric is proposed for head-to-head comparison of different or future schemes. Furthermore, some schemes such as symmetric double-sided two-way ranging (SDS-TWR) [14] depend on specially chosen timings for the best performance, while others such as the alternative double-sided two-way ranging (AltDS-TWR), first shown in [5] and later adopted in [8], achieve similar performance without any timing constraints. In practical systems, lack of precise timing control may limit the accuracy, flexibility, and scalability of a localization scheme. Existing works ignore such differences. Fulfilling this gap, our work proposes a metric that can capture both the best-achievable accuracy, and the dependency on operating conditions (or lack thereof), providing clear comparison between any ranging scheme. Of course, there might exist other points of comparison, such as the number of messages exchanged or who computes the final distance, but we have instead concentrated only on the ranging error due to clock drifts.

II. Clock Drift Error Analysis

Any newly proposed ranging scheme must be analyzed for its robustness to clock-drifts. To demonstrate how such analysis is performed, we derive the error due to clock drift in detail for the SDS-TWR scheme[1]. The following notations are commonly used: ρ_{AB} represents the propagation delay, or time of flight (ToF) between A and B. T_{AB} represents the time difference of arrival (TDoA) of tag T's message at two anchors A and B: $T_{AB} = \rho_{BT} - \rho_{AT}$.

[1]Note that this analysis is not our contribution. Hence, we will not perform similar analysis for the other 6 schemes we examine in this paper.

A. Symmetric double-sided two-way ranging (SDS-TWR)

In SDS-TWR [14], a pair of UWB ranging devices exchange POLL-RESP-FIN messages (see Figure 1). The response times D_A and D_B are the delays between reception of a previous message and the transmission of the next one. R_A and R_B are round-trip times. The ToF between A and B can be calculated [14] as

$$\rho_{AB} = \frac{1}{4}(R_A - D_A + R_B - D_B).$$

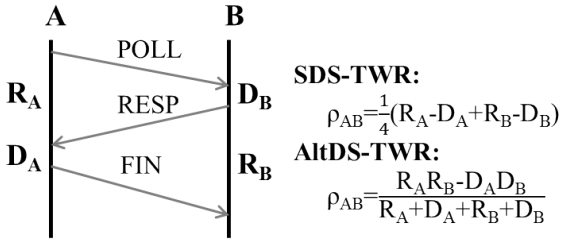

Fig. 1: Message exchanges in SDS-TWR and AltDS-TWR

B. Error Analysis for SDS-TWR

Since R_A, R_B, D_A, and D_B are all based on internal clocks, they are subject to drifts. Consequently, the measured time interval deviates from the true interval by: $\hat{R}_A = (1 + \delta_A)R_A, \hat{D}_A = (1 + \delta_A)D_A, \hat{R}_B = (1 + \delta_B)R_B, \hat{D}_B = (1+\delta_B)D_B$, where δ_A and δ_B are the clock drift rates for the two devices defined as the amount of timing drift per unit time. Measured ToF ($\hat{\rho}_{AB}$) minus the true ToF (ρ_{AB}) represents the clock drift ranging error:

$$\hat{\rho}_{AB} - \rho_{AB} = \frac{1}{4}[(R_A - D_A)\delta_A + (R_B - D_B)\delta_B].$$

Substituting $R_A = D_B + 2\rho_{AB}$, $R_B = D_A + 2\rho_{AB}$:

$$\hat{\rho}_{AB} - \rho_{AB} = \frac{1}{2}(\delta_A + \delta_B)\rho_{AB} + \frac{1}{4}(\delta_A - \delta_B)(D_B - D_A).$$

Two observations can be made from this error expression:

- The first term is very small. With worst case clock drift around $\delta_A = \delta_B = 20$ ppm, this term amounts to sub-picosecond errors, and is therefore practically ignored.
- Theoretically, the second term can be reduced to zero if $|D_B - D_A| = 0$, meaning, SDS-TWR error is *dependent* on careful control of the response times.

These observations indicate that SDS-TWR can achieve low ranging error only so long as the two turn-around times are equal—a careful implementation is thus required.

We now introduce 6 other ranging schemes that we will evaluate using our metric. These schemes are the single-sided two-way ranging (SS-TWR) [14], the alternative double-sided two-way ranging (AltDS-TWR) [8], the passive extended two-way ranging (PE-TWR) [9], the passive extended two-way ranging with alternative calculation (AltPE-TWR) [15], the Djaja-Josko and Kolakowski method (DJKM) [16], and the Double Pulsed Whistle (DPW) [10]. The detailed derivations

of range equations and clock drift errors will not be included but can be found in the cited works, and they follow the similar procedures as described above for SDS-TWR. All 7 schemes serve as examples for how the metric we developed can be used to evaluate and compare different schemes.

C. Single-sided two-way ranging (SS-TWR)

SS-TWR [14] only utilizes first two messages of SDS-TWR. With only measurements of D_B and R_A (Figure 1), it calculates ρ_{AB} with a simple formula:

$$\rho_{AB} = \frac{1}{2}(R_A - D_B).$$

With clock drifts, the timing error is

$$\hat{\rho}_{BT} - \rho_{BT} = \rho_{AB}\delta_A + \frac{1}{2}(\delta_A - \delta_B)D_B.$$

The first term is negligible since it is only a fraction of a pico-second. However, the second term is significant as the response delay D_B cannot be made arbitrarily small because of hardware limitations (radio turnaround, processor speed, etc.). Usually, D_B is in the order of milliseconds, and the second term could cause tens of centimeters to several meters of error. Unlike SDS-TWR, this term cannot be cancelled, and therefore SS-TWR suffers from clock drift induced errors.

D. The AltDS-TWR scheme

The AltDS-TWR [8] is proposed to improve upon SDS-TWR. Surprisingly, the message exchange in AltDS-TWR (Figure 1) is exactly the same as SDS-TWR. The only difference is the formula used for computing ρ_{AB}, which enables its key advantage over SDS-TWR. The ToA, ρ_{AB}, can be calculated by:

$$\begin{aligned}\rho_{AB} &= \frac{R_A R_B - D_A D_B}{2(R_A + D_A)} \\ &= \frac{R_A R_B - D_A D_B}{2(R_B + D_B)} \\ &= \frac{R_A R_B - D_A D_B}{R_A + R_B + D_A + D_B}\end{aligned}$$

With clock drifts, the error of the ToA measurement is:

$$\begin{aligned}\hat{\rho}_{AB} - \rho_{AB} =& \delta_A \rho_{AB}, \\ \text{OR} \quad & \delta_B \rho_{AB}, \\ \text{OR} \quad & \frac{\delta_A + \delta_B + 2\delta_A\delta_B}{2 + \delta_A + \delta_B}\rho_{AB} \approx \frac{\delta_A + \delta_B}{2}\rho_{AB},\end{aligned}$$

depending on which ranging equation is used. This quantity is very small, but unlike SDS-TWR, it does not depend on terms like D_A and D_B, meaning it achieves low error regardless of system configurations.

E. The PE-TWR scheme

In PE-TWR [9], a tag device performs SDS-TWR messaging with an anchor A. Another anchor B, which overhears the communication between the tag and anchor A, can calculate its ToA to the tag, assuming the distance between the anchors is previously known (Figure 2). With the measured time intervals

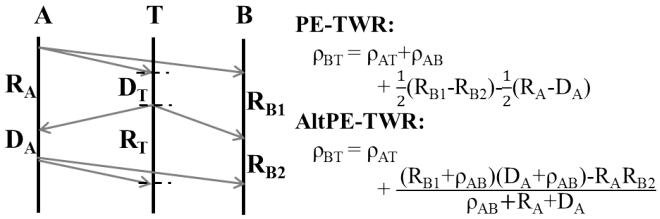

Fig. 2: Message exchanges in PE-TWR and AltPE-TWR

$R_A, D_A, R_T, D_T, R_{B1}$, and R_{B2} shown in Figure 2, the ToA between the tag and anchor B, ρ_{BT} can be calculated as:

$$\rho_{BT} = \rho_{AT} + \rho_{AB} + \frac{R_{B1} - R_{B2}}{2} - \frac{R_A - D_A}{2}.$$

The corresponding error when considering clock drift is:

$$\begin{aligned}&\hat{\rho}_{BT} - \rho_{BT} \\ &\quad = \frac{1}{2}\left((\delta_B + \delta_A)(T_{AB} - \rho_{AB}) + (\delta_B - \delta_A)(R_{B1} - D_A)\right).\end{aligned}$$

The first term is again negligibly small. The second term can become significant because it involves response delay D_A, which is in the order of milliseconds. Similar to SDS-TWR, by constraining the response time such that $D_A = D_T$, this term can be brought close to propagation delay making the second term very small, thus achieving good error performance.

F. The AltPE-TWR Scheme

The AltPE-TWR [15] is an improved version of PE-TWR, which follows the same communication protocol (Figure 2) as PE-TWR. However, the method of calculating ρ_{BT} is modified:

$$\rho_{BT} = \frac{(R_{B1} + \rho_{AB})(D_A + \rho_{AB}) - R_A R_{B2}}{\rho_{AB} + R_A + D_A} + \rho_{AT}.$$

The error due to clock drift can be derived as:

$$\hat{\rho_{BT}} - \rho_{BT} = \delta_B(T_{AB} - \rho_{AB}) + \frac{R_A \rho_{AB}(\delta_B - \delta_A)}{\rho_{AB} + R_A + D_A}.$$

Denoting $k = \frac{\rho_{AB}+R_A+D_A}{R_A} = \frac{D_A+D_T+2\rho_{AT}+\rho_{AB}}{D_T+2\rho_{AT}} \approx \frac{D_A+D_T}{D_T}$, the error can be approximated as $\hat{\rho_{BT}} - \rho_{BT} \approx \delta_B(T_{AB}-\rho_{AB}) + \frac{\rho_{AB}(\delta_B-\delta_A)}{k}$. Both terms are negligibly small with any practical value for k. Unlike PE-TWR, AltPE-TWR does not impose any constraint on D_A and D_T.

G. The Djaja-Josko and Kolakowski method (DJKM)

DJKM [16] is a TDoA ranging scheme proposed by Djaja-Josko and Kolakowski. A pair of anchors A and B perform normal SDS-TWR, while the tag device can calculate its TDoA to A and B just by overhearing the SDS-TWR messages and measuring the time intervals R_{T1} and R_{T2} between each message (Figure 3). Assuming that ρ_{AB} is known beforehand, the TDoA, T_{AB}, can be computed as:

$$T_{AB} = R_{T1} - D_B - \rho_{AB},$$

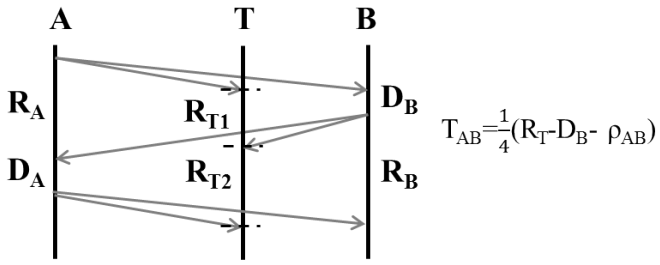

Fig. 3: Message exchanges in DJKM

where R_{T1} is the time interval from the tag receiving POLL to the tag receiving RESP. Considering clock drift, the timing error can be calculated as:

$$\hat{T}_{AB} - T_{AB} = \delta_T(\rho_{AB} + T_{AB}) + (\delta_T - \delta_B)D_B.$$

Similar to SS-TWR, the second term is significant and cannot be reduced due to hardware limitations.

H. The DPW Scheme

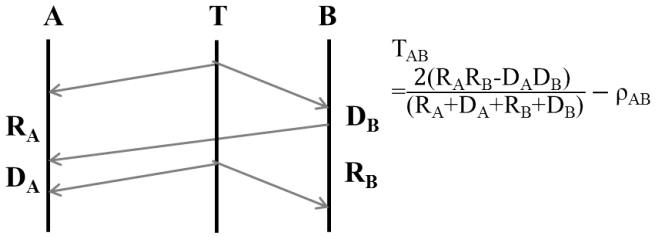

Fig. 4: Message exchanges in DPW

The DPW scheme [10] is another TDoA ranging scheme where the communication is initiated by the tag and received by anchors A and B. Upon receiving this message, anchor B responds after a certain amount of delay D_B. The tag then sends a second message received by A and B (Figure 4). With the measurements of the time interval D_A, D_B, R_A, and R_B, the TDoA of the tag to anchors A and B can be calculated with:

$$\begin{aligned} T_{AB} &= \frac{(R_A R_B - D_A D_B)}{R_A + D_A} - \rho_{AB} \\ &= \frac{(R_A R_B - D_A D_B)}{R_B + D_B} - \rho_{AB} \\ &= \frac{2(R_A R_B - D_A D_B)}{R_A + D_A + R_B + D_B} - \rho_{AB}. \end{aligned}$$

If the time measurements are affected by clock drift, the error in the TDoA calculation is

$$\begin{aligned} \hat{T}_{AB} - T_{AB} =& \delta_A T_{AB} + \delta_A \rho_{AB}, \\ \text{OR} \quad & \delta_B T_{AB} + \delta_B \rho_{AB}, \\ \text{OR} \quad & (T_{AB} + \rho_{AB}) \frac{\delta_A + \delta_B + 2\delta_A\delta_B}{2 + \delta_A + \delta_B}, \\ \approx & (T_{AB} + \rho_{AB}) \frac{\delta_A + \delta_B}{2}, \end{aligned}$$

depending on which formula is used. The error is negligibly small regardless of the choice of system parameters.

Table I summarizes the error expressions for 7 schemes that we compare in this work. It is interesting to note how older schemes that depended on a system property such as equal D_A and D_B were eventually improved upon. Our proposed E-G metric simplifies visualizing this difference.

III. Our E-G Metric

We propose a metric formulated as a 2-tuple, $\langle E, G \rangle$, where E numerically embodies the best-achievable error despite clock drift, and G measures the error's dependence on response times. Each scheme, represented by its own E-G tuple, can then be plotted on a 2D plane to compare with others. The appropriate numerical values are assigned based on realistic simulation results. Their derivation and rationale are described below. Note that the E-G metric can be obtained numerically without first having an analytical error equation.

A. Minimum Error (E-metric)

In the $\langle E, G \rangle$ tuple, E is representative of the minimum magnitude of timing error when the response time of the ranging device pair is chosen optimally. For example, in the case of SDS-TWR, to obtain E, we would assume that $D_A = D_B$ such that the error due to clock drift is the most optimized. Since clock-drifts are not in our control, in our simulation, we find the clock-drift pair that induces the *worst* minimum error. In general, suppose S is the scheme under examination, $\mathbf{D} = \{D_A, D_B, ...\}$ is the set of response time configured in the devices in the system, and $\mathbf{\Delta} = \{\delta_A, \delta_B, ...\}$ is the set of clock drift rates affecting the devices. Then metric E is defined as:

$$E(S) = \max_{\mathbf{\Delta}} \left(\min_{\mathbf{D}} \left(|e(S, \mathbf{D}, \mathbf{\Delta})| \right) \right), \tag{1}$$

where $e(S, \mathbf{D}, \mathbf{\Delta})$ is defined as the timing error given that the devices in the system have the set of response time and clock drift rates specified by $\mathbf{D}$ and $\mathbf{\Delta}$:

$$e(S, \mathbf{D}, \mathbf{\Delta}) = M - GT, \tag{2}$$

where M and GT denote the measured value (affected by clock drifts) and the ground truth value respectively.

Algorithm 1 shows the numerical simulation to find $E(S)$.

B. Dependency on Response Time (G-metric)

The second part of the tuple, G, is representative of how dependent the error is on the response times. When $e(S = s, \mathbf{D}, \mathbf{\Delta})$ is plotted as a function of $\mathbf{D}$, it defines a scheme-dependent surface (see Figure 5). We observe that the e function of schemes like AltDS-TWR, with no constraints on response time, defines a plane parallel to the horizontal plane, while schemes that are dependent on the response times define a sloped plane. Thus, observing the slope provides intuitions about how quickly the results deviate from the optimum, as the response times deviate from the best system settings. We define, G as the magnitude of e's gradient:

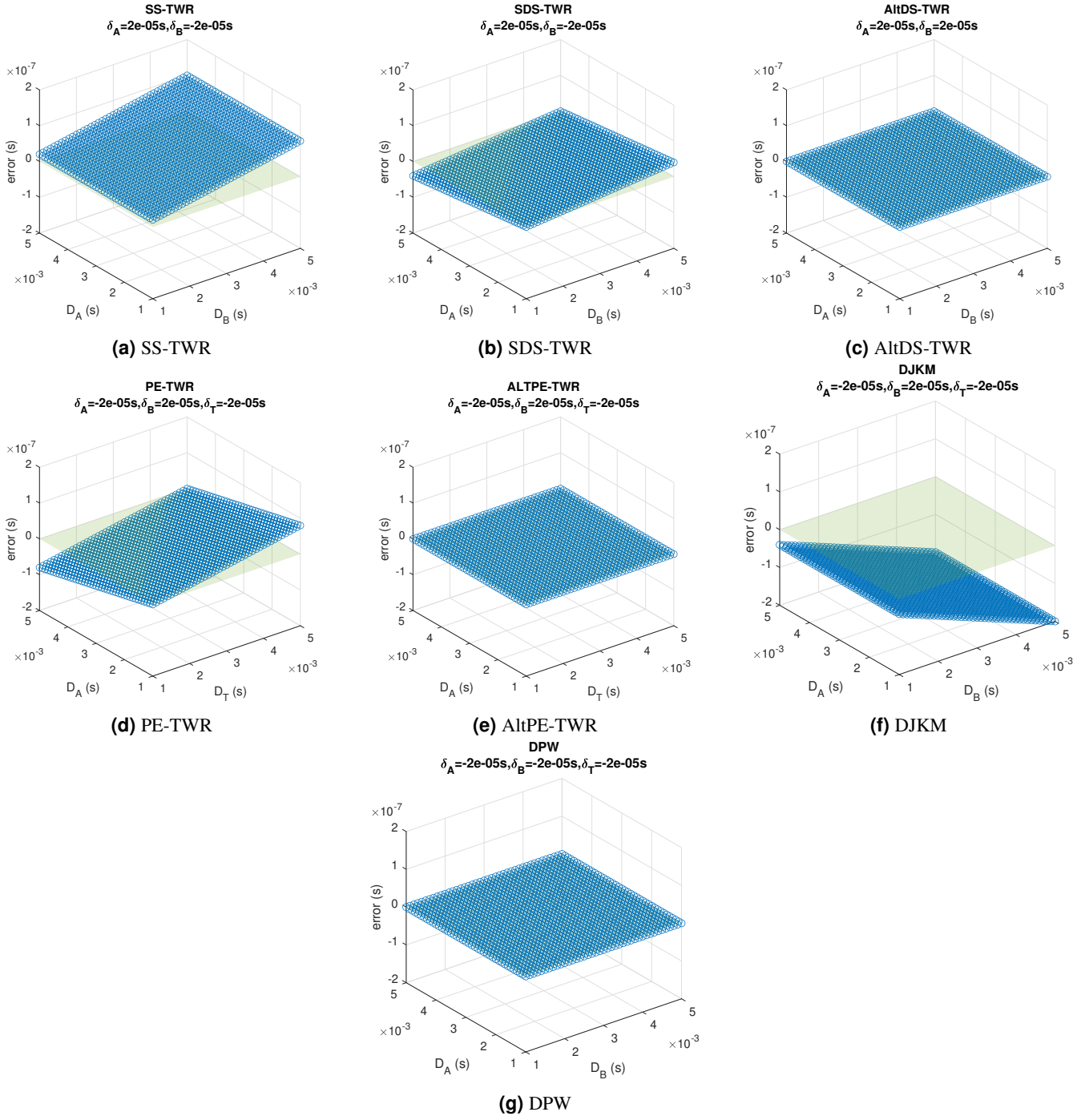

(a) SS-TWR **(b)** SDS-TWR **(c)** AltDS-TWR

(d) PE-TWR **(e)** AltPE-TWR **(f)** DJKM

(g) DPW

Fig. 5: Timing error vs. response time (light-green is reference 0-plane; simulation step size=0.1 ms) [2]

$$G(S) = \max_{\delta_1,\delta_2,\ldots,\delta_N} \sqrt{\sum_{i=1}^{N} \left(\frac{de}{dD_i}\right)^2}, \tag{3}$$

where, N is the number of devices, and D_i is the response time of the i^{th} such device. If all devices do not transmit response messages, we treat those devices' $\frac{de}{dD_i}$ as 0, with no influence on the value of G.

[2]In order to have consistent axes, the D_A axis in Figure 5 is retained for SS-TWR and DJKM although they only have one device that transmits response message.

Ranging Method	**Scheme**	**E (s)**	**G**	**Error Expression**
ToA	SS-TWR	2.0000×10^{-8}	2.0000×10^{-5}	$\rho_{AB}\delta_A + \frac{1}{2}(\delta_A - \delta_B)D_B$
	SDS-TWR	6.6713×10^{-14}	1.4142×10^{-5}	$\frac{1}{2}\rho_{AB}(\delta_A + \delta_B) + \frac{1}{4}(\delta_A - \delta_B)(D_B - D_A)$
	AltDS-TWR	6.6713×10^{-14}	0	$\delta_A\rho_{AB}$
	PE-TWR	2.6685×10^{-13}	2.8284×10^{-5}	$\frac{1}{2}((\delta_A + \delta_B)(T_{AB} - \rho_{AB}) + (\delta_A - \delta_B)(D_A - R_{B1}))$
	AltPE-TWR	2.6685×10^{-13}	5.3902×10^{-11}	$\delta_B(T_{AB} - \rho_{AB}) + \frac{R_A\rho_{AB}(\delta_B - \delta_A)}{\rho_{AB}+R_A+D_A}$
TDoA	DJKM	4.0000×10^{-8}	4.0000×10^{-5}	$\delta_T(\rho_{AB} + T_{AB}) + (\delta_T - \delta_B)D_B$
	DPW	1.3343×10^{-13}	0	$\delta_A T_{AB} + \delta_A\rho_{AB}$

TABLE I: The E-G Metric for the six ranging schemes under consideration.

Algorithm 1 Algorithm for computing E metric

for each $\mathbf{\Delta}$ combination **do**
  for each $\mathbf{D}$ combination **do**
    GT := The actual ρ_{AB} (ToA), or T_{AB} (TDoA).
    Compute the measured timing intervals assuming the system is affected by clock drifts with the set of drift rates, $\mathbf{\Delta}$.
    M := Find the measured ToA or TDoA based on the measured timing intervals with clock drift.
    $e := M - GT$
  end for
  e' := min(e) minimum over $\mathbf{D}$
end for
return E := max(e') maximum over $\mathbf{\Delta}$

C. Simulation method

According to the IEEE standard [14], the response time is on the order of several milliseconds. In our simulation, we assume the range of response time is between $1 - 5\,ms$, which is typical for practical systems. Due to the delay associated with packet processing, packet formation, and radio switching, the response time cannot be easily decreased below $1\,ms$. Larger than $5\,ms$ response times are not typical since ranging schemes cannot tolerate device mobility during the process. We use the maximum permissible clock drift rates of ± 20 ppm to elicit the worst-case error. Designers of future ranging schemes are of course free to assume any values.

IV. Results and Discussion

The E-G metric computed for 7 UWB ranging schemes is shown in Table I. The simulation assumes clock drift for all devices within ± 20 ppm. The devices are assumed to be $1\,m$ apart for 2-device schemes. For 3-device schemes, two anchors are located at (-2,0) and (1,0), and the tag is located at (0,0). The locations are configurable, but do not significantly impact the result for short distances. The ranging error computed with different configurations of response time offer the following observations (refer to Figure 5):

1) **The slope of the plane** visualizes the underlying operating principles of the ranging scheme (blue). A horizontal plane (as in AltDS-TWR and DPW), indicates that the error is independent of the response times. The sloping plane for SS-TWR and DJKM indicates error dependency on only one of the ranging devices, while the diagonally sloping plane crossing the zero-plane for SDS-TWR and PE-TWR indicates error dependency on response times of both devices. Error diminishes when the response times fall on the diagonal line. Therefore, SS-TWR and DJKM require *small response times*, whereas SDS-TWR and PE-TWR require devices to exhibit *equal response times*.
2) **The minimum magnitude of error** can be observed from the lowest point of different graphs. Among evaluated schemes, SS-TWR and DJKM have the worst error performance, since, practically, the response time cannot be reduced below $1\,ms$.

The E-G metric allows plotting the 7 ranging schemes on a single 2D plot (see Figure 7, and Table I). The most superior scheme would be located at the bottom-left corner with the lowest minimum error and no dependencies on system response times. AltDS-TWR [5], AltPE-TWR [15], and DPW [10] exhibit this behavior and are the best schemes under our analysis. Any scheme located to the right will have a higher minimum error, lowering the ranging accuracy. A scheme higher on the y-axis has higher response-time dependency—choice of response time easily influences accuracy for these schemes.

The timing error does depend on the physical distance between devices since ρ and T feature in the error equations. Figure 6a shows the influence on the E and G values as we change the distance from $1\,m$ to $10\,m$ for 2-device schemes, and for 3-device schemes, the first anchor is moved across $(-2, 0)$ to $(-12, 0)$. Observe that G is invariant over distance, whereas E increases with distance. However, this variation is quite negligible (Figure 6b), to the tune of ≈ 1 picosecond ($< 1\,mm$). It does not warrant consideration in the E-G metric.

The E-G metric shows great potential for analysing and comparing any ToA and TDoA schemes. The advantage is especially exemplified in AltPE-TWR (section II-F) where it is difficult to derive a clean expression for timing error. Without clever manipulation of the error expression, it can be difficult to get any intuition on the error performance. With the E-G metric, error is computed numerically and directly compared to other scheme, making the E-G metric a useful tool for speeding up the invention of new schemes and establishing a benchmark for comparing ranging schemes.

One drawback of the E-G metric is that the dependency term only includes the configured response delay of the UWB devices. However, we contend that the system response delay

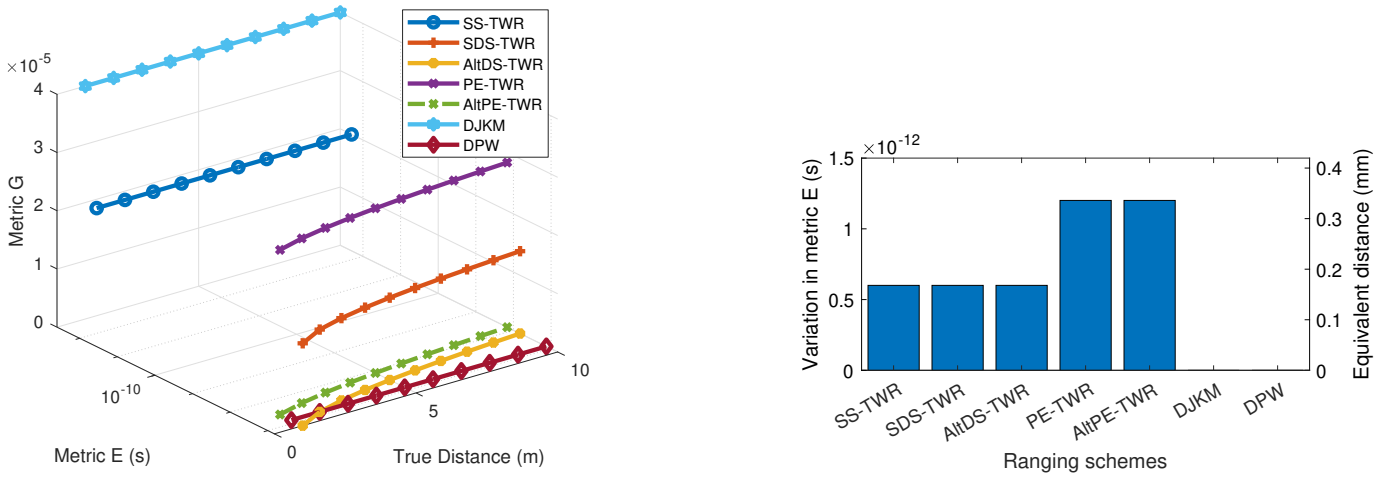

(a) Variation of E-G metric over distance of 1-10 meters

(b) Amount of variation in metric E with changing distance

Fig. 6: Distance dependency of E-G values

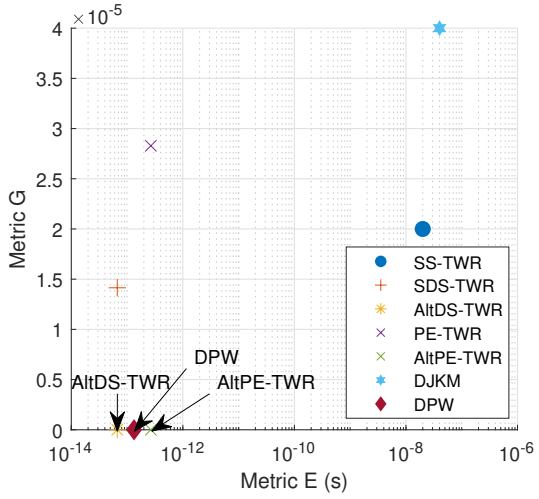

Fig. 7: Comparison of different schemes by E-G metric

is the most fundamental factor to the error caused by clock drift. We leave a more comprehensive metric for future works.

V. Implications and Conclusion

Ranging schemes that do not have dependencies on the choices of response time are desirable since it might be impossible to ensure those constraints. From a protocol design standpoint, constraints on response time limit flexibility. For example, if a ranging scheme relies on broadcasts [17]–[19], ensuring equal response time for every device-pair is difficult. We envision that future works will analyse their system using the E-G metric when creating new ranging schemes.

The effects of synchronization error: There exist several TDoA protocols that require synchronization among anchor devices [20], [21]. To analyse these protocols, clock drift is of less importance to the ranging precision as the devices' clocks and time measurements are being constantly corrected for. Rather, the synchronization accuracy and timestamping resolution have more impact in the ranging error, which depends on the specific synchronization medium (wired or wireless), synchronization protocol and frequency, and hardware specifications. In our analysis, we only consider synchronization-free ranging protocols.

The use cases of E-G metric: We envision the E-G metric can be used by researchers and industry for the following purposes. (1) *Analysing future ranging schemes*: when coming up with a new ranging protocol, researchers can quickly verify the robustness of their protocol against existing methods by plotting their E-G metric on Fig. 7. (2) *Choosing the right ranging protocol*: it is likely that a mobile device capable of indoor localization is also involved in other sensing, computation, and communication tasks. Therefore, guaranteeing the exact timing of ranging message responses is difficult [18]. The E-G metric can help system designers to choose the most robust ranging protocol that performs well under unpredictable or varying response time. (3) *Choosing the right parameters*: some applications require a certain mode of localization, e.g. a system that requires the mobile device to localize without exposing itself to the infrastructure needs to use a passive-tag protocol, like DJKM. Our analysis in Fig. 5 can help the system designer to understand how different system parameters such as response time affect localization performance, and choose the appropriate value for a specific application. (4) *Fusion of multiple protocols*: in some cases, it's helpful to fuse the localization results from different protocols to produce a better location estimate. The E-G metric can help with calculating the level of uncertainty of each protocol as a useful input to the fusion algorithm.

In conclusion, E-G metric provides analytically consistent numerical analysis of clock-drift induced ranging error in localization schemes, and through our 2-tuple metric simplifies comparisons. Demonstrating the usefulness of the E-G metric, we show a comparison of seven existing ranging schemes, and

hope that future schemes will be compared with the state-of-the-art using our open-source metric.

REFERENCES

[1] Locatify, "What is the new apple u1 chip, and why is it important?" https://locatify.com/blog/what-is-the-new-apple-u1-chip-and-why-is-it-important/, 2020.

[2] K. Kim, "Samsung expects UWB ... the next big wireless technologies," https://bit.ly/3jHHv0S, 2020.

[3] X. Team, "Xiaomi introduces groundbreaking uwb technology," https://bit.ly/3JauVEs, 2020.

[4] A. Developer, "Google adds ultra-wideband (uwb) api to android with focus on smart homes," https://bit.ly/3qpFaeI, 2020.

[5] D. Neirynck, E. Luk, and M. McLaughlin, "An alternative double-sided two-way ranging method," *WPNC 2016*, 2017.

[6] V. Sark, N. Maletic, M. Ehrig, J. Gutiérrez, and E. Grass, "Achieving millimeter precision distance estimation using two-way ranging in the 60 ghz band," in *2019 European Conference on Networks and Communications (EuCNC)*, 2019, pp. 310–314.

[7] N. Maletic, V. Sark, M. Ehrig, J. Gutiérrez, and E. Grass, "Experimental evaluation of round-trip tof-based localization in the 60 ghz band," in *2019 International Conference on Indoor Positioning and Indoor Navigation (IPIN)*, 2019, pp. 1–6.

[8] IEEE802.15.4z, "Ieee standard for low-rate wireless networks–amendment 1: Enhanced ultra wideband (uwb) physical layers (phys) and associated ranging techniques," *IEEE Std 802.15.4z-2020 (Amendment to IEEE Std 802.15.4-2020)*, pp. 1–174, 2020.

[9] K. A. Horvath, G. Ill, and A. Milankovich, "Passive extended double-sided two-way ranging algorithm for UWB positioning," *ICUFN*, 2017.

[10] M. Von Tschirschnitz and M. Wagner, "Synchronization-Free and Low Power TDOA for Radio Based Indoor Positioning," *IPIN 2018*, 2018.

[11] K. Mikhaylov, A. Tikanmaki, J. Petajajarvi, M. Hamalainen, and R. Kohno, "On the selection of protocol and parameters for UWB-based wireless indoors localization," *ISMICT*, 2016.

[12] C. L. Sang, M. Adams, T. Hörmann, M. Hesse, M. Porrmann, and U. Rückert, "An Analytical Study of Time of Flight Error Estimation in Two-Way Ranging Methods," *IPIN 2018*, 2018.

[13] M. von Tschirschnitz, M. Wagner, M.-O. Pahl, and G. Carle, "Clock Error Analysis of Common Time of Flight based Positioning Methods," *IPIN 2019*, 2019.

[14] IEEE802.15.4, "Ieee standard for local and metropolitan area networks–part 15.4: Low-rate wireless personal area networks (lr-wpans)," *IEEE Std 802.15.4-2011 (Revision of IEEE Std 802.15.4-2006)*, 2011.

[15] K. A. Horvath, G. Ill, and A. Milankovich, "Passive extended double-sided two-way ranging with alternative calculation," *2017 IEEE 17th International Conference on Ubiquitous Wireless Broadband, ICUWB 2017 - Proceedings*, vol. 2018-Janua, pp. 1–5, 2018.

[16] V. Djaja-Josko and J. Kolakowski, "A new transmission scheme for wireless synchronization and clock errors reduction in UWB positioning system," *IPIN 2016*, 2016.

[17] Y. Cao, A. Dhekne, and M. Ammar, "6Fit-A-Part: A Protocol for Physical Distancing on a Custom Wearable Device," *ICNP 2020*, 2020.

[18] A. Dhekne, A. Chakraborty, K. Sundaresan, and S. Rangarajan, "Trackio: Tracking first responders inside-out," *NSDI 2019*, 2019.

[19] A. Dhekne, U. J. Ravaioli, and R. R. Choudhury, "P2ploc: Peer-to-peer localization of fast-moving entities," *Computer*, vol. 51, no. 10, 2018.

[20] M. Stocker, B. Großwindhager, C. A. Boano, and K. Römer, "SnapLoc: an ultra-fast UWB-based indoor localization system for an unlimited number of tags," in *Proceedings of the 18th International Conference on Information Processing in Sensor Networks*. New York, NY, USA: ACM, apr, pp. 348–349.

[21] A. Ledergerber, M. Hamer, and R. D'Andrea, "A robot self-localization system using one-way ultra-wideband communication," in *2015 IEEE/RSJ International Conference on Intelligent Robots and Systems (IROS)*, vol. 2015-Decem. IEEE, sep 2015, pp. 3131–3137. [Online]. Available: http://ieeexplore.ieee.org/document/7353810/